EFFICIENT THERMALLY CONDUCTIVE STRAP DESIGN FOR CRYOGENIC PROPELLANT TANK SUPPORTS AND PLUMBING

J.P. Elchert, R. Christie
NASA Glenn Research Center

P. Gebby
Vantage Systems, Inc.

A. Kashani
Atlas Scientific

C. Opalach
Lewis Educational and Research Collaborative Internship Program

ABSTRACT

After evaluating NASA space architecture goals, the Office of Chief Technologist identified the need for developing enabling technology for long term loiters in space with cryogenic fluids. One such technology is structural heat interception. In this prototype, heat interception at the tank support strut was accomplished using a thermally conductive link to the broad area cooled shield. The design methodology for both locating the heat intercept and predicting the reduction in boil-off heat leak is discussed in detail. Results from the chosen design are presented. It was found that contact resistance resulting from different mechanical attachment techniques played a significant role in the form and functionality of a successful design.

PROBLEM

The Cryogenic Boil-off Reduction System team utilized heat interception at the multilayer insulation, tank support struts, and plumbing lines. The primary heat exchanger was the broad area cooled shield, which existed in an optimal location in the multilayer insulation. A reverse turbo Brayton cycle cryocooler operated at roughly 80 K to actively cool this shield and a thermally conductive link was required to connect the broad area cooling tubes to the strut. This requirement raised the question of how to locate the minimum mass thermal link on the strut such that a maximum amount of heat was removed.

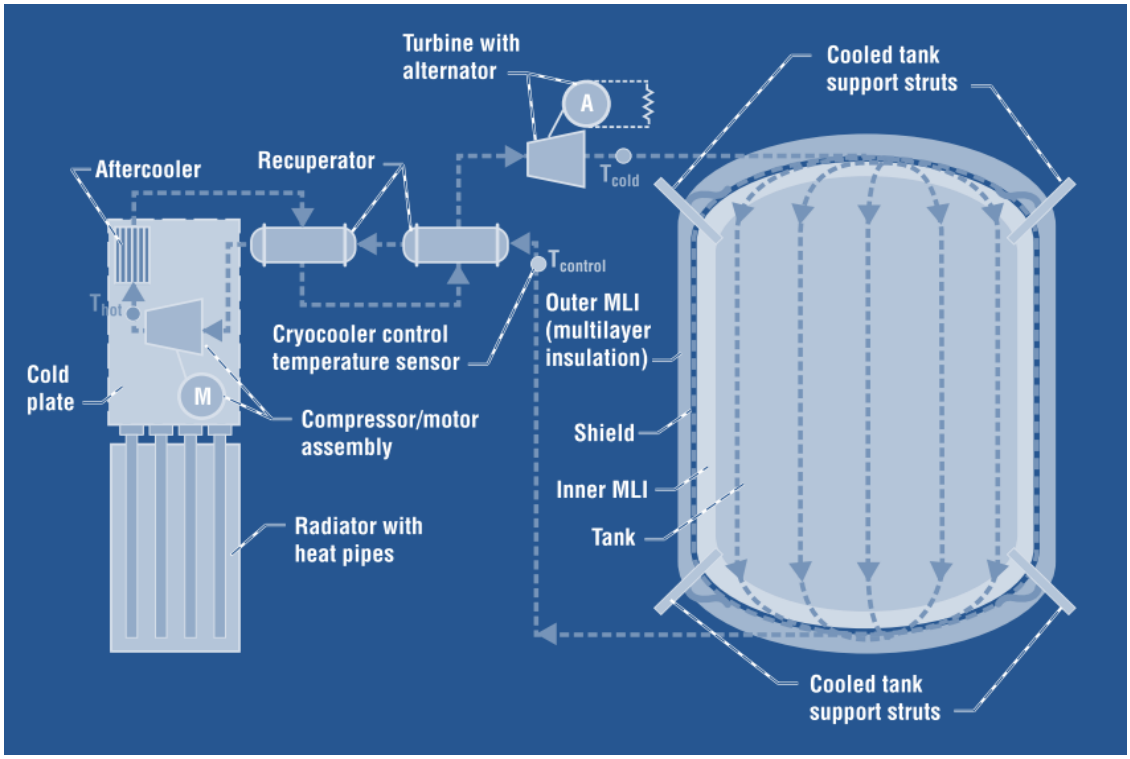

Figure 1. Schematic of the cryogenic boil-off reduction system test

Thermal conductance is a logical place to start because it is directly related to the size (and mass) of the link,

$$G = \frac{kA}{L} \approx \frac{km}{\rho L^2}$$

where *G* is the thermal conductance, *L* is the length of the link, *k* is the material thermal conductivity, and *A* is the link cross-sectional area. Assuming that the area to length ratio is roughly equal to the volume divided by the square of the length, the proportionality to the mass of the link, m is obvious (density is ρ). This coupling of conductance and mass motivates an optimum design that achieves an allowable conductance without increasing the link mass excessively.

PROCEDURE

The design methodology was composed of four simple steps:

1. Sizing with simple, idealized model
2. Detailed design with performance checks
3. Validate with most detailed model
4. Troubleshoot and re-design

The first step in finding an optimal design was to determine the minimum thermal conductance that would supply the desired heat removal. Ideal thermal models of varying conductances of a hypothetical thermal link from a boundary to the strut were generated to examine the heat removed. Parameters of the thermal model used can

be found in Table 1. The location of the heat removal node was then swept along the length of the strut or plumbing line.

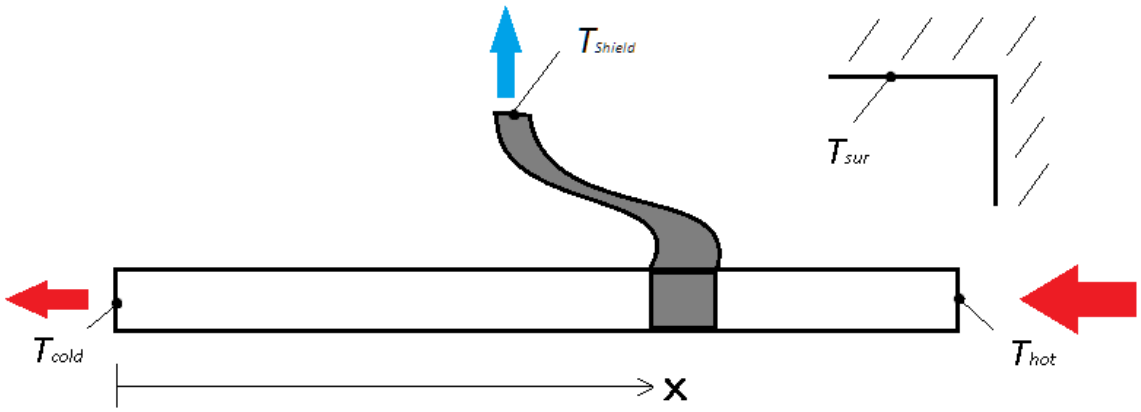

Figure 2. Depicted here is a schematic of the basic thermal link problem. In the simple sizing model, the thermal radiation was neglected.

Table 1. Model Parameters

Parameter	Symbol	Value
Hot Boundary Temperature	T_h	225 K
Cold Boundary Temperature	T_c	20.23 K
Cooled BAC Shield Temperature	T_{BAC}	78.9 K

In this manner it was found that as the conductance was increased, the additional heat removed diminished to zero. The effect can be seen in Figure 3 in which the heat removed by the intercept and the heat leak into the tank are plotted against the position of the intercept for various thermal link conductances. A key assumption in Figure 3 is that the thermal link and the strut make perfect contact with no thermal losses. This assumption will be relaxed later.

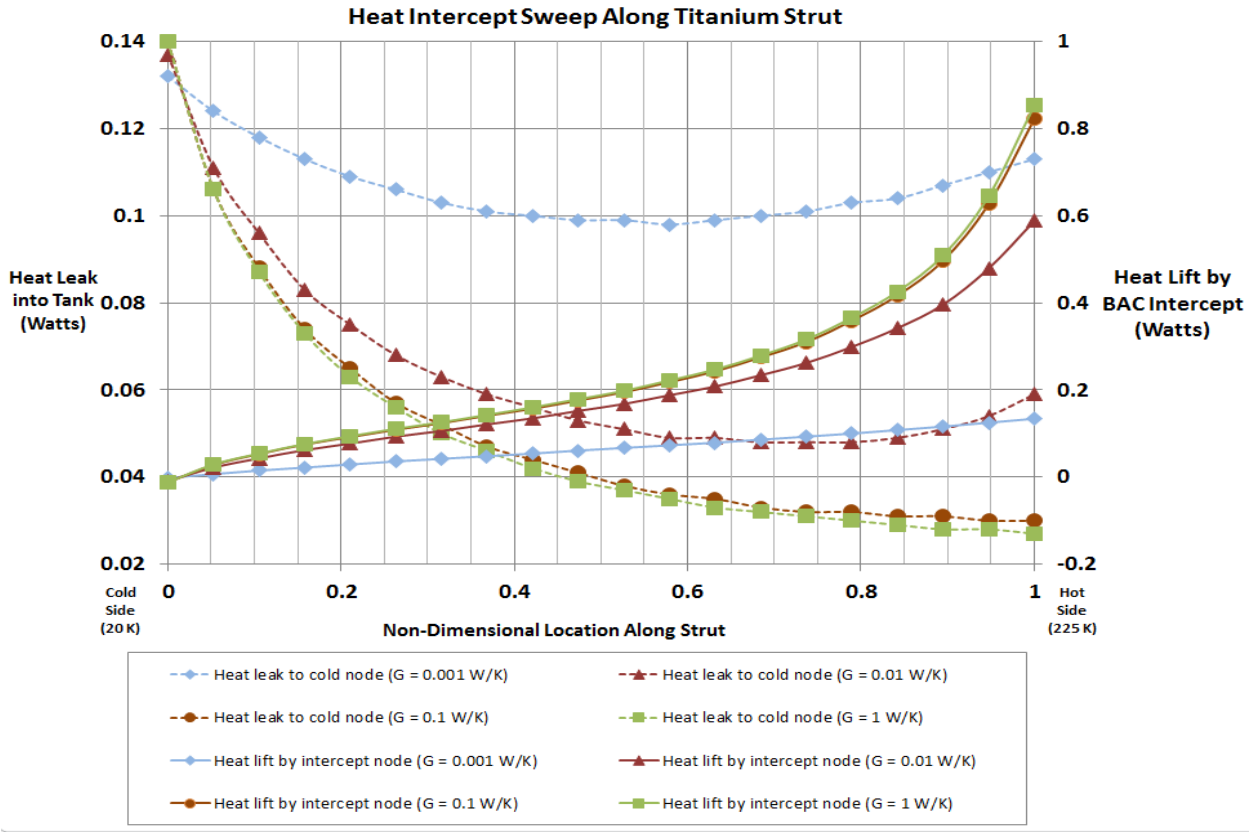

Figure 3. This plot illustrates the diminishing effectiveness of increasing thermal link conductivity. Here, the dotted lines use the left axis and the solid lines use the right axis. Just to be clear, the last data point is erroneously shown as finite; really, the solution goes to infinity because the intercept node is coincident with the hot boundary node.

From the information shown in Figure 3, a conductance value of 0.1 W/K was selected as a target on the basis that greater values would increase the mass while not offering a significant improvement on the design.

After finding the required size, the next step was to actually define the dimensions. Bugby and Marland explain an accepted approach in the Spacecraft Thermal Control Handbook, Volume 2, which was adapted to this problem (1).

$$G = \frac{k_{mean} W N t}{(L/\eta_s)} \eta_e$$

Here, the thermal conductivity was evaluated at 85K, which was a good estimate for its temperature. W was the width, N the number of layers, t the layer thickness, L the typical shortest distance between attachment points, and η_s the shape efficiency. The so-called shape efficiency arises because at this stage, engineers were uncertain about the final length of the link. It was used as, essentially, a rule of thumb to estimate how much longer the real link needed to be to actually attach the two points of interception. It was assumed that $\eta_s = 0.7$ and $L = 7\ inches$. It was found through trial and error that bus bar composed of three layers of 1 mm by 20 mm copper would result in the desired conductance of 0.1 W/K—assuming the end piece efficiency, $\eta_e = 1$.

The components used in the original heat intercept design are shown in Figure 4. The thermal link depicted was bus bar made of three layers of copper wrapped in an insulating rubber. In final assembly, the rubber insulation was removed.

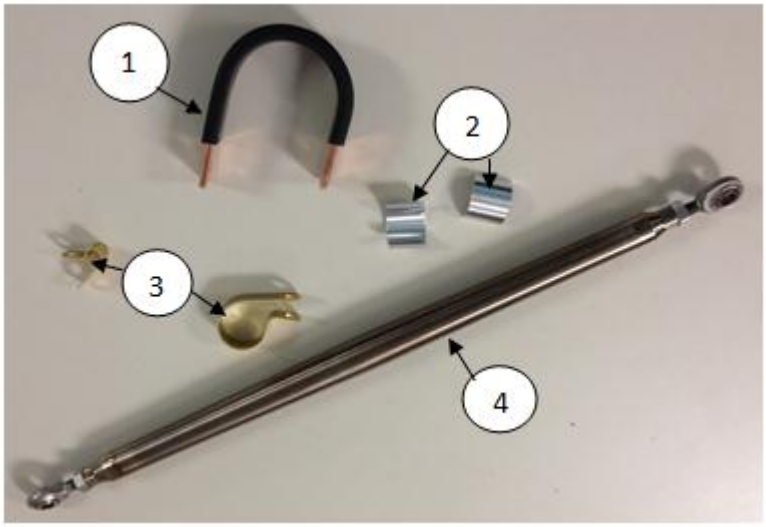

Figure 4. Heat intercept components of the original design are shown here; bus bar (1), aluminum collars (2), loop clamps (3) and the strut (4).

In reality, the sizing analysis should reflect the total conductance of the system connecting strut and BAC shield. These connections provide an additional loss of conductivity; a result of imperfect contact. This loss was modeled and the results are reflected in Figure 6. By examining the differences between Figure 3 and Figure 6 it was concluded that the original clamp design seen in Figure 4 resulted in a contact resistance that was too great to allow an acceptable total conductance. In hindsight, the end piece efficiency should have been assumed to be $\eta_e = 0.45$, with contact resistances being evaluated using FEA surface pressures and contact resistances evaluated with Kumar and Ramamurthi's work on low temperature pressed contacts (2).

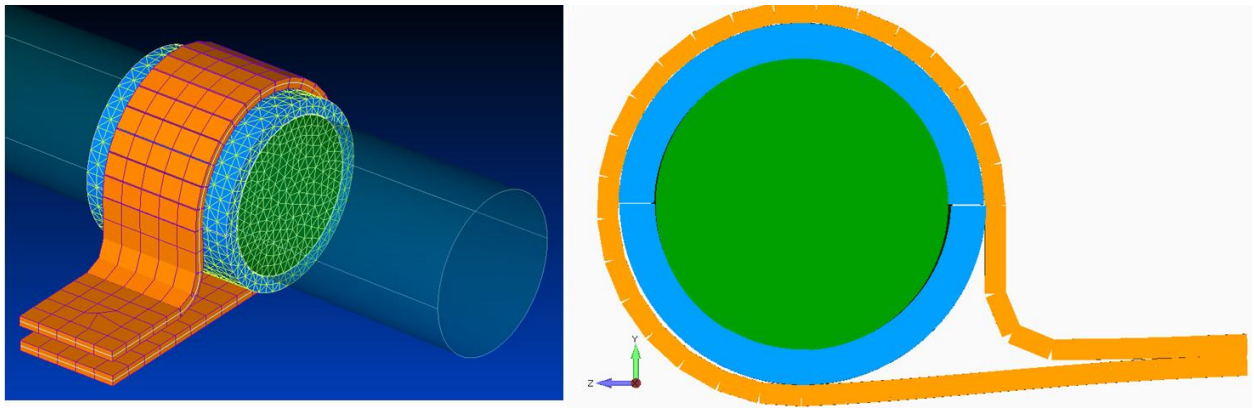

Figure 5. Shown here is finite element analysis of the original design by P. Gebby. It was demonstrated that the loop clamp could not make even contact, as shown by the gaps between the aluminum sleeve and the loop clamp in the deformed geometry (right), necessitating re-design.

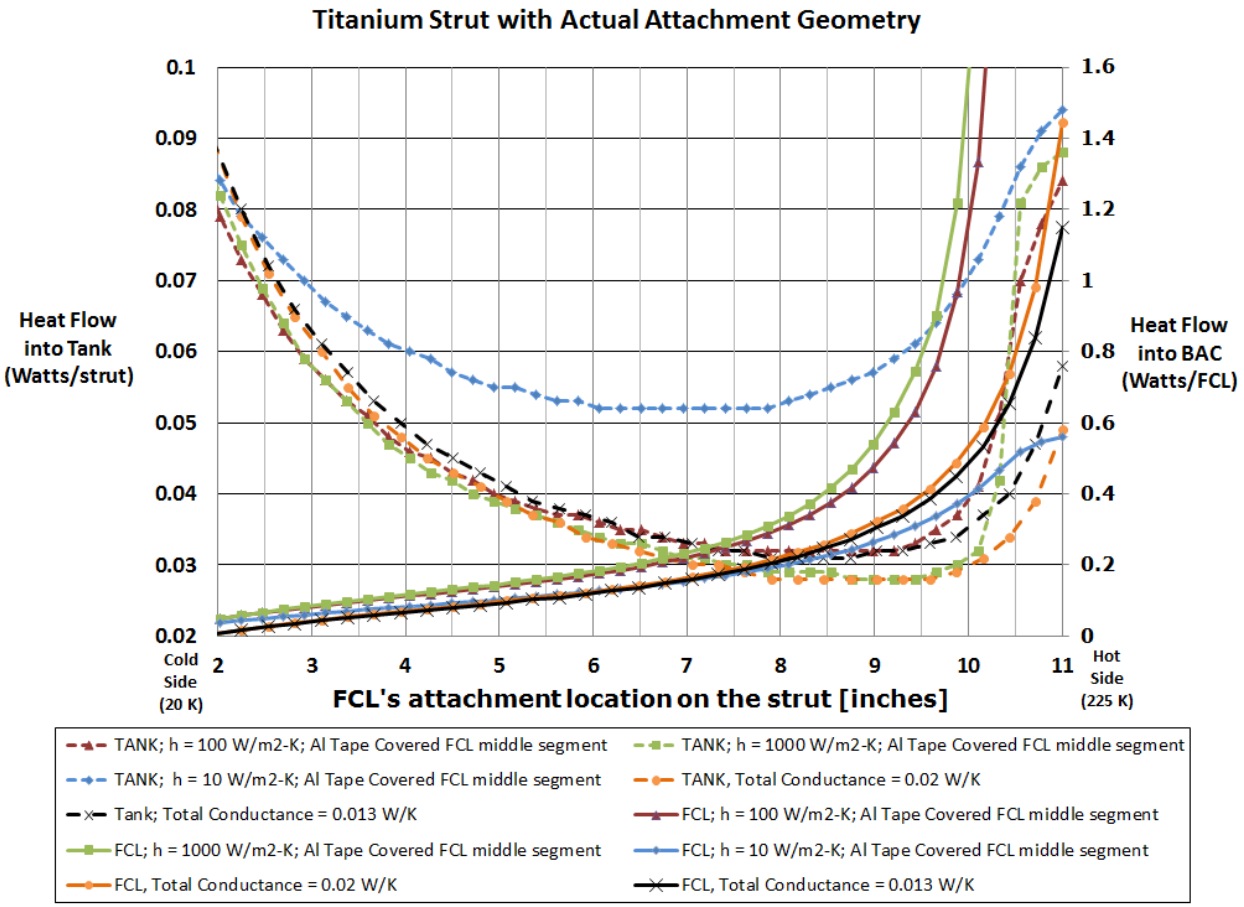

Figure 6. Heat intercept sweep with actual surface contact modeled shows the effect of poor contact on the system. These plots were generated with a detailed finite difference model including thermal radiation at 220K.

To remedy this situation a new clamp design was created that increased the surface of contact as shown in Figure 7. In addition to the improved clamp, the contact resistance was improved through the use of indium foil positioned between clamp and tube. One rule of thumb is to use indium foil between interfaces of different materials and Apiezon type N grease between interfaces of the same material. With the new design, a conductance of 0.045 W/K was attainable.

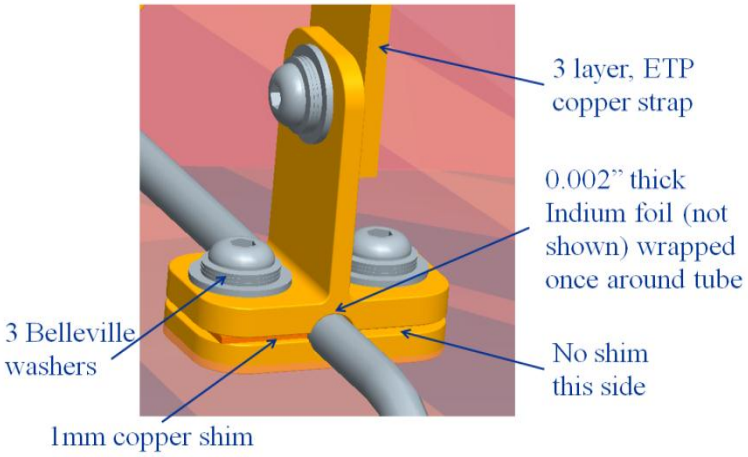

Figure 7. Improved clamp interface.

Figure 8 shows the incorporation of the thermal connections in the whole tank model. It is important to note that the links are not able to take the shortest direct path between structures. This additional length requirement in not negligible and had to be accounted for in the analysis in the performance of the thermal links.

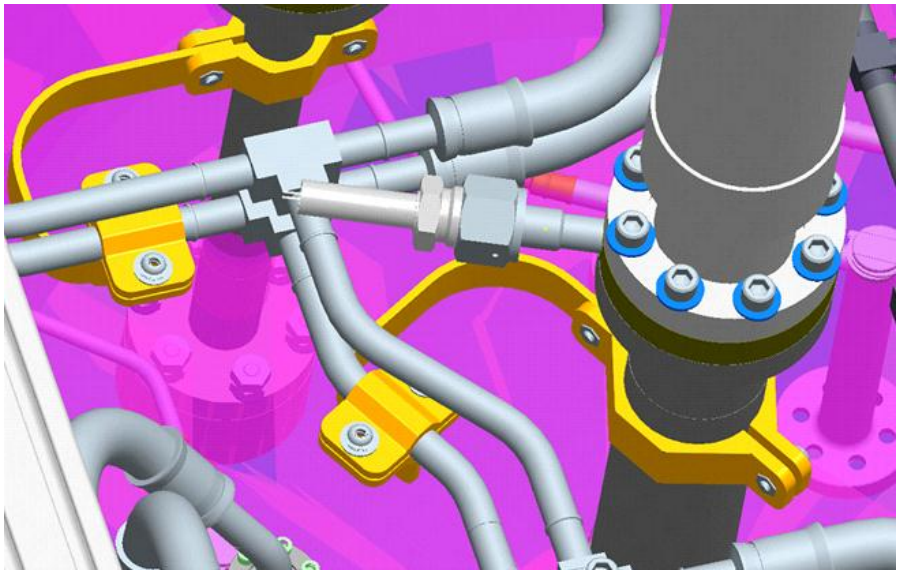

Figure 8. Connections from BAC Shield plumbing to stainless steel vent plumbing

RESULTS

Without cooling, co-author Ali Kashani found the steady state strut heat leak to be roughly 0.6 W. With the cooling straps, a reduction in strut heat leak of roughly 70% was predicted (down to 0.16 W). When compared to an infinitely conductive link, this design had a fin efficiency of over 90%. Finally, if it could be repeated, the team would start by assuming an end piece efficiency of 0.45 to approximately capture the effect of the contact resistance.

It is useful to point out that the temperature change was roughly 10K—which seems large to the uninitiated. These results show that performance is not a strong function of temperature change across the link so long as one is free to locate the link anywhere along the length of the strut.

Also, in this case, the mass was only about 0.25 kg per link. Even though, for this prototype, it was effective and economical to use the bus bar link, in future thermal link designs, for peak performance, engineers should use a flexible foil copper thermal link with contiguous end piece design. This would eliminate the contact resistance between the copper strap and the end piece, effectively changing $\eta_e = 0.45$ to roughly $\eta_e = 0.8$.

CONCLUSIONS

A reasonable conductance could be achieved while keeping the mass involved to a minimum. The design methodology also demonstrated the importance of considering contact resistances existing in the final system.

ACKNOWLEDGEMENTS

The authors would like to acknowledge the Cryogenic Propellant Storage and Transfer team for its support throughout the design process. The authors would also like to give a special thanks to the Lewis Educational and Research Collaborative Internship Program (LERCIP).

REFERENCES

1. Bugby, D., and B. Marland. "Flexible Conductive Links." *Spacecraft Thermal Control Handbook*. Ed. Maritn Donabedian. Vol. II. El Segundo, California: Aerospace, 2003. 337-38. Print. Cryogenics.

2. Kumar, S. Sunil, and K. Ramamurthi. "Thermal Contact Conductance of Pressed Contacts at Low Temperatures." Cryogenics 44 (2004): n. pag. Print.

3. Guzik, M. Cryogenic boil-off reduction system poster. (2012)